Bubble Columns for Condensation at High Concentrations of Noncondensable Gas: Heat-Transfer Model and Experiments

G. Prakash Narayan
Dept. of Mechanical Engineering, Massachusetts Institute of Technology, Cambridge, MA 02139

Mostafa H. Sharqawy
Dept. of Mechanical Engineering, King Fahd University of Petroleum and Minerals, Dhahran, Saudi Arabia

Steven Lam
Dept. of Mechanical Engineering, Massachusetts Institute of Technology, Cambridge, MA 02139

Sarit K. Das
Dept. of Mechanical Engineering, Indian Institute of Technology-Madras, Chennai, India

John H. Lienhard V
Dept. of Mechanical Engineering, Massachusetts Institute of Technology, Cambridge, MA 02139

DOI 10.1002/aic.13944
Published online February 8, 2013 in Wiley Online Library (wileyonlinelibrary.com).

Carrier gas based thermodynamic cycles are common in water desalination applications. These cycles often require condensation of water vapor out of the carrier gas stream. As the carrier gas is most likely a noncondensable gas present in very high concentrations (60–95%), a large additional resistance to heat transfer is present. It is proposed to reduce the aforementioned thermal resistance by condensing the vapor–gas mixture in a column of cold liquid rather than on a cold surface using a bubble column heat exchanger. A theoretical predictive model for estimating the heat-transfer rates and new experimental data to validate this model are described. The model is purely physics based without the need for any adjustable parameters, and it is shown to predict heat rates within 0 to −20% of the experimental values. The experiments demonstrate that heat-transfer rates in the proposed device are up to an order magnitude higher than those achieved in existing state-of-the-art dehumidifiers. © 2013 American Institute of Chemical Engineers *AIChE J,* 59: 1780–1790, 2013
Keywords: condensation, bubble column, noncondensable gas, thermal resistance model, dehumidification, moist air, carrier gas

Introduction

When a noncondensable gas is present, the thermal resistance to condensation of vapor on a cold surface is much higher than in a pure vapor environment. This is, primarily, due to the diffusion resistance to transport of vapor through the mixture of noncondensable gas and vapor. Several researchers have previously studied and reported this effect.[1–9] There is a general consensus that, when even a few mole percent of noncondensable gas is present in the condensing fluid, the deterioration in the heat-transfer rates could be up to an order of magnitude.[10–15] From experimental reports in the literature, it can be observed that the amount of deterioration in heat transfer is a very strong (almost quadratic) function of the mole fraction of noncondensable gas present in the condensing vapor. For this reason, a deaerator is usually used in power plants to prevent the accumulation of noncondensable gas in the steam condenser. However, in other applications, including water desalination, the presence of air in steam condensation is not always avoidable.

In desalination systems using air as a carrier gas, a large percentage of air (60–95% by mass) is present in the condensing stream. As a consequence, it has been found that, in these systems, the heat exchanger used for condensation of water out of an air–vapor mixture (otherwise known as dehumidifier) has very low heat-transfer coefficients (as low as 1 W/m^2 K in some cases[16,17]). In this article, we propose to improve the heat-transfer rate by condensing the vapor–gas mixture in a column of cold liquid rather than on a cold surface using a bubble column heat (and mass) exchanger.

Bubble columns are extensively used as multiphase reactors in process, biochemical, and metallurgical applications.[18] They are used especially in chemical processes involving reactions that have a very high heat release rate associated with them (such as the Fischer–Tropsch process used in the manufacture of synthetic fuels).[19,20] We propose to apply this device for condensation of the air–vapor mixture with a large percentage of air present in it. Figure 1 illustrates the proposed device schematically. In this device, moist air is sparged through a porous plate (or any other

Correspondence concerning this article should be addressed to J. H. Lienhard V at lienhard@mit.edu.

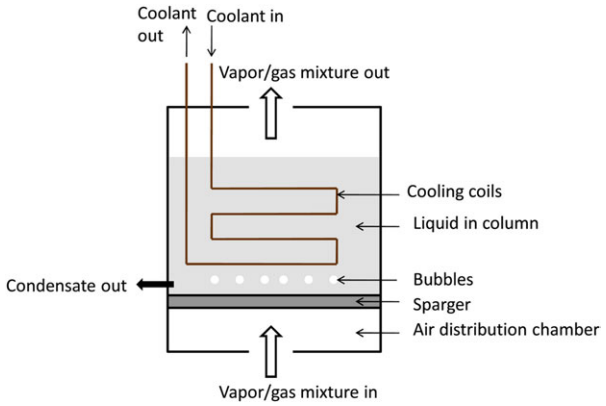

Figure 1. Schematic diagram of the bubble column dehumidifier.

[Color figure can be viewed in the online issue, which is available at wileyonlinelibrary.com]

type of sparger[21]) to form bubbles in a pool of cold liquid. The upward motion of the air bubbles causes a wake to be formed underneath the bubble that entrains liquid from the pool, setting up a strong circulation current in the liquid pool.[22] Heat and mass are transferred from the air bubble to the liquid in the pool in a direct contact transport process. At steady state, the liquid, in turn, loses the energy and it has gained to the coolant circulating through a coil placed in the pool for the purpose of maintaining the liquid pool at a steady temperature.

Predictive Model for Combined Heat and Mass Transfer

In this section, we develop a thermal resistance model for the condensation of water from an air–vapor mixture in a bubble column heat exchanger. Figure 2 illustrates a local thermal resistance network describing the heat- and mass-transfer processes in the bubble column condenser. To draw this network, we define local energy-averaged "bulk" temperatures for the condensing mixture, the liquid in the pool, and the coolant and also approximate the heat transfer to be locally one-dimensional.

The four temperature nodes in the network are: (1) the average local temperature of the air–vapor mixture in the bubbles (T_{air}), (2) the average temperature of the liquid in the pool (T_{column}), (3) the local temperature of the coil surface (T_{coil}), and (4) the average local temperature of the coolant inside the coil ($T_{coolant}$). Between T_{air} and T_{column}, there is direct contact heat and mass transfer. The heat transfer is via a thermal resistance represented by $R_{sensible}$ and the mass transfer is represented as a (latent) heat source ($q_{lt} = j \cdot h_{fg}$). The thermal resistance due to the coil wall itself will be very small and has been neglected. This is especially true in the cases considered in this article, as copper tubing is used. In cases where stainless steel or a lower thermal conductivity metal is used, this resistance might not be negligible. Between the coil surface and the bubble, there could be direct contact heat exchange and associated condensation of vapor on the coil surface. The heat transfer is via a heat-transfer resistance R_{impact}, and the mass transfer is represented by the heat source $q_{lt,impact}$. Several researchers[19,20,23–25] have previously studied the thermal resistance between the pool of liquid and the immersed surface in a bubble column reactor. In the this article, this resistance is represented as R_{bc} between T_{coil} and T_{column}. Finally, there is a convective resistance inside the coil for the coolant flow represented by R_{coil}.

To simplify the circuit, the direct impact of the bubble on the coil surface is approximated to have negligible effect on the heat and mass transfer (i.e., R_{impact} and $q_{lt,impact}$ are neglected). The experiments were designed and carried out such that this approximation was satisfied (see "Experimental Details" section), and the effect of direct impact was dealt with in a separate set of experiments (see "Effect of Bubble-on-Coil Impact" section). Each of the remaining resistances depicted above will be modeled using reasonable simplifying assumptions in the following paragraphs.

Thermal resistance between the liquid in the column and the coil surface

In bubble column reactors used in the chemical industry, proper design of the heat-transfer surfaces is vital to maintain catalytic activity, reaction integrity, and product quality, because the reactions typically involve very high heat release rates because of their highly exothermic or endothermic nature. In these scenarios, the temperature of the liquid in the column is of utmost importance. Hence, several studies have been conducted over the last five decades on modeling and measuring the heat-transfer coefficients between the liquid and the heat-transfer surface.

In a pioneering effort, Konsetov[24] proposed a semianalytical model based on the assumption that heat rates are determined by isotropic turbulent fluctuations in the liquid. He approximated the characteristic dimension for heat transfer from the liquid to the coil to be the coil diameter and used the Kutateladze model[26] for determining the gas holdup. Konsetov used a flexible constant to fit the data from the model to experimental data in the literature. This correlation, however, has not been widely used for bubble column reactor design.

Kast[25] developed a model by considering that a fluid element in front of the rising bubble receives radial momentum and moves toward the wall. This was postulated to break up the boundary layer at the wall. The author proposed that below the bubble, liquid is sucked in at a radial velocity V_r and that this results in a capacitive heat transport given by $V_r \cdot \rho \cdot c_p$. He further observed that V_r is proportional to the superficial gas velocity V_g and defined Stanton number as $St = \frac{h}{\rho_l \cdot c_{p,l} \cdot V_g}$. Based on intuitive reasoning, Kast proposed the following correlation

$$St = f(ReFrPr)^n \tag{1}$$

Deckwer[23] used the Kolmogorov theory of isotropic turbulence[27] and Higbie's theory of surface renewal[28] to explain

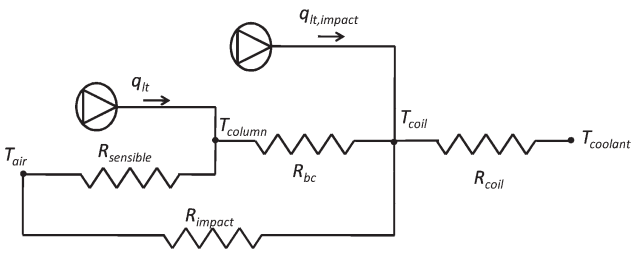

Figure 2. A thermal resistance model for the bubble column dehumidifier.

the form of the equation (Eq. 1) proposed by Kast. By observing that there is no experimental evidence of a physical length scale for the heat transfer, Deckwer postulated that the microeddy scale of energy dissipation (see Eq. 2) proposed by Kolmogorov is an ideal characteristic length scale for the problem at hand. The author also proposed use of the Kolmogorov velocity (see Eq. 3) as the characteristic velocity.

$$l = \left(\frac{\nu^3}{\varepsilon}\right)^{1/4} \tag{2}$$

$$V = (\nu\varepsilon)^{1/4} \tag{3}$$

The heat-transfer correlation (Eq. 4), thus, derived by Deckwer had the same form as Kast's model and used a flexible constant.

$$St = c(ReFrPr)^{-0.25} \tag{4}$$

In a separate publication,[29] the present authors have described an improved model for predicting the heat-transfer rate between the liquid in the column and the coil surface. In this model, we (like Deckwer[23]) used Higbie's theory of surface renewal, however, with a different length scale. In fluid elements adjacent to the surface, unsteady heat diffusion takes place and is described by the following equation

$$\frac{\partial T}{\partial t} = \alpha \frac{\partial^2 T}{\partial x^2} \tag{5}$$

The appropriate boundary conditions to describe this problem are ones that describe the temperature T as the wall temperature T_{coil} at $x = 0$ and all times, the bubble temperature as the initial temperature at all x, and T as the bubble temperature at $x = \infty$ at all times. The final boundary condition is possible only when we approximate the fluid element to have infinite depth and the contact times to be short.

$$T = T_{\text{coil}} \quad x = 0 \quad t \geq 0 \tag{6}$$

$$T = T_{\text{bubble}} \quad x > 0 \quad t = 0 \tag{7}$$

$$T = T_{\text{bubble}} \quad x = \infty \quad t > 0 \tag{8}$$

Solving the above equations, we can obtain the following expression for the heat flux and the thermal resistance.

$$q = \frac{2}{\sqrt{\pi}} \sqrt{\frac{k\rho c_{\text{p}}}{t}} \cdot (T_{\text{bubble}} - T_{\text{coil}}) \tag{9}$$

$$\frac{1}{R_{\text{bc}}} = \frac{2}{\sqrt{\pi}} \sqrt{\frac{k\rho c_{\text{p}}}{t}} \tag{10}$$

From Eq. 10, it is clear that the resistance can be modeled by modeling the surface renewal time (t). For modeling t, we need to model the characteristic length scale and velocity scale accurately. As stated earlier, Deckwer modeled the length and velocity using the Kolmogorov theory (Eqs. 2 and 3). These scales are indicative of the smallest eddies present in the flow and are the scales at which energy is dissipated. These are the scales that form the viscous sublayer and are very small physically. Hence, this scale is unlikely to regulate the surface renewal mechanism and the physical mixing. We propose to use a more intuitive length scale that is the integral scale of turbulence.

The integral scale is the representative size of the largest energy bearing eddy. In some cases, this scale can be defined by the physical constraints of the flow domain. For example, in pipe flow, the diameter of the pipe is of the order of the largest eddies in the flow, and the ratio of the pipe diameter to mean velocity along the pipe is a good estimate of the time period required to describe the flow. In other cases where the integral scale is not obvious from the flow geometry, it can be defined using the autocorrelation of the velocity (i.e., the correlation of a velocity component with itself) as follows

$$l_{\text{int}} = \int_0^{\infty} \frac{u(x,t) \cdot u(x+r,t)}{u^2} dr \tag{11}$$

where u is the root-mean-square velocity in the x-direction and r is the distance between two points in the flow. The determination of the integral scale using Eq. 11 is not straight-forward.[30–32] Direct numerical simulations or large-scale visualization experiments using particle image velocimetry or other such techniques are normally used to obtain the autocorrelation of velocity in a 3D flow like in bubble columns.[33] Instead of going into these elaborate techniques, we propose to approximate the integral scale by the bubble diameter. Magaud et al.[34] have presented experimented data that support this approximation. Similar results, concluding that the integral length is of the order of the bubble diameter, have been reported by other authors as well.[35,36]

We have presented various expressions to calculate the bubble diameter (depending on flow regime) in a previous publication.[29] We use the following expression for the cases involved in this article.[37]

$$D_{\text{b}} = \left\{\frac{6\sigma d_{\text{o}}}{(\rho_{\text{l}} - \rho_{\text{g}}) \cdot g}\right\}^{1/3} \tag{12}$$

We also propose to use the liquid circulation velocity as the characteristic velocity. This is logical, because the liquid that "renews" the boundary layer formed on the heat-transfer surface is at this velocity, and when we aim to calculate the time between two "renewals" we need to take this into account. Field and Rahimi[38] have proposed that the following expression, which is commonly used in the literature,[20] is appropriate to calculate liquid circulation velocity in bubble columns.

$$V_{\text{c}} = 1.36\left\{gH(V_{\text{g}} - \epsilon \cdot V_{\text{b}})\right\}^{1/3} \tag{13}$$

According to this expression, the circulation velocity is a function of the bubble velocity, and we have previously presented various expressions for calculating the same.[29] An appropriate correlation from the wide selection needs to be picked based on the conditions in the bubble column. For the cases reported in this article, we find it appropriate to use the following equation for evaluating bubble velocity developed based on Mendelson's wave equation.[39] Our own experimental observations showed that this correlation works well for the cases reported in this publication.

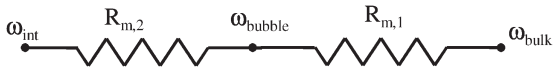

Figure 3. A mass-transfer resistance model between the liquid in the column and the bubbles.

$$V_b = \sqrt{\frac{2\sigma}{\rho_l D_b} + \frac{gD_b}{2}} \tag{14}$$

To calculate circulation velocity based on Eq. 13, we also need to evaluate the volumetric gas holdup (ϵ), for which we propose to use the following expression provided by Joshi and Sharma.[22] Several other correlations that have been reported by various researchers, but for the conditions under which we conducted the experiments (described in "Experimental Details" section), we find the following correlation to be the most appropriate. Also, we find that this correlation (Eq. 15) is the most widely used by researchers in the field. Our own experimental observations showed that this correlation works well for the cases reported in this publication.

$$\epsilon = \frac{V_g}{0.3 + 2 \cdot V_g} \tag{15}$$

Based on these expressions, we can evaluate the time between two renewals as $t = \frac{D_b}{V_c}$. By applying this contact time to Eq. 10, we evaluate the thermal resistance between the liquid in the column and the coil surface. We have previously presented a comparison of the model presented here to the experimental values in the literature, and there is excellent agreement.[29] This resistance is, however, a minor one in the network, and the prediction of the same has little effect on the overall result for the cases reported in this publication.

Thermal resistance between the liquid in the column and the bubbles

The high resistance to diffusion of vapor through a vapor–gas mixture is the reason that regular dehumidifiers have low heat-transfer coefficients. In this section, we model the equivalent of the aforementioned diffusion resistance for the case of bubble column dehumidifiers. In Figure 2, the total heat flux between the bubbles and the liquid was modeled as the sum of the heat flux due to condensation (q_{lt}) and the heat flux due to heat transfer through the resistance $R_{sensible}$. We will evaluate the latent heat using a mass-transfer resistance model and the sensible heat using a heat- and mass-transfer analogy. The mass-transfer resistances associated with condensation are shown in Figure 3. In drawing these resistances, it is approximated that the condensation occurs at an interface just outside the bubble surface and mass-averaged bulk humidity ratios are defined for the vapor–gas mixture inside the bubble and at the bubble interior surface.

The mass-transfer resistances depicted in Figure 3 are: (1) the resistance to diffusion of vapor through the vapor–gas mixture ($R_{m,1}$) in the bulk (ω_{bulk}) to the bubble surface (ω_{bubble}) and (2) the mass-transfer resistance caused by bubble motion through the liquid ($R_{m,2}$). The first resistance is not easy to model without knowing the mechanism of convective transport inside the bubble, which could be augmented by a fluid circulation caused by rapid and asymmetric vertical motion of the bubble in the liquid pool. As there are several complexities involved in evaluating the mechanism of transport inside the bubble, we assume a boundary layer is formed for diffusive transport and approximate the thickness of the boundary layer by the radius of the bubble itself. This is an upper limit for the size of the boundary layer and the associated thermal resistance, and hence, in the succeeding sections ("Comparison of Model and Experiments" section), it is shown that the heat transfer and condensation rates predicted by the model consistently underestimate those measured experimentally. The model equation is

$$k_{l,1} = \frac{D_{AB}}{D_b/2} \tag{16}$$

We model the resistance outside the bubble surface using surface renewal mechanism (similar to that presented in Eqs. 5–10)

$$k_{l,2} = \frac{2}{\sqrt{\pi}}\sqrt{\frac{D_{AB}}{t}} \tag{17}$$

The surface renewal time (t) in this case is modeled as the ratio of the bubble diameter and the bubble slip velocity. The bubble slip velocity is the relative velocity of the bubble with respect to the circulating liquid. The liquid circulation velocity and the bubble velocity are calculated using the expression presented in Eqs. 13 and 14, respectively. The model equation is

$$t = \frac{D_b}{V_b - V_c} \tag{18}$$

The heat-transfer resistance $R_{sensible}$ can be modeled by defining Lewis factor (Le_f) for the vapor–gas system. The Lewis factor appears in the governing equations of simultaneous heat and mass-transfer processes (e.g., in wet-cooling towers[40] and in cooling coils[41]). Le_f is defined by Eq. 19 and is directly related to Lewis number, which is a fluid property

$$Le_f = \frac{h_t}{k_l \rho c_{pg}} \tag{19}$$

$$Le_f \cong Le^{2/3\ 41} \tag{20}$$

$$\approx 089-092 \text{ for air}-\text{water systems}^{42} \tag{21}$$

$$Le = \frac{\alpha}{D_{AB}} \tag{22}$$

where h_t is the heat-transfer coefficient associated with $R_{sensible}$, k_l is the mass-transfer coefficient associated with the latent heat, and c_{pg} is the specific heat at constant pressure of the vapor–gas mixture

$$\frac{1}{h_t A} = R_{sensible} \tag{23}$$

$$\frac{1}{k_l} = \left(\frac{1}{k_{l,1}} + \frac{1}{k_{l,2}}\right)^{-1} \tag{24}$$

Here, the heat- and mass-transfer coefficients are defined based on the heat-transfer area of the coil surface (A) instead of the bubble surface area. This is because from an engineering perspective, we need to evaluate the coil area required for a certain total heat duty in the bubble column dehumidifier.

Finally, the correlations for heat-transfer coefficient for flow inside circular tubes are well known and documented in heat-transfer text books.[43] Based on the flow regime inside the coil, we selected appropriate correlations to evaluate R_{coil}.

Evaluation of total heat flux from the resistance model

In the preceding sections, we discussed the models for the various thermal resistances in the bubble column dehumidifier (Figure 2). In this section, we present the equations needed to solve for the total heat flux and all the temperatures in the bubble column dehumidifier.

The heat flux through the network associated with the sum of the bubble column resistance (R_{bc}) and the convection resistance in the coil (R_{coil}) is defined as follows

$$q = \frac{\dot{Q}}{A} \tag{25}$$

$$= \frac{\theta_1}{R_{bc} + R_{coil}} \tag{26}$$

The associated log mean temperature difference (θ_1) is defined between the liquid column temperature (T_{column}) and the coolant inlet/exit temperatures. It is very important to note that experimental data in the literature and our own experimental data reported later in this article (see "Experimental Details" section) have shown the liquid in the column is at a constant temperature because of rapid mixing induced by the bubbles. The logarithmic mean temperature difference (LMTD) is given as follows

$$\theta_1 = \frac{(T_{column} - T_{coolant,in}) - (T_{column} - T_{coolant,out})}{\ln\left(\frac{T_{column} - T_{coolant,in}}{T_{column} - T_{coolant,out}}\right)} \tag{27}$$

The heat flux can also be expressed as sum of the latent heat of condensation of the vapor from the vapor–air bubbles into the liquid column and the associated sensible heat transfer.

$$q = q_{latent} + q_{sensible} \tag{28}$$

The sensible heat flux is the one associated with the resistance $R_{sensible}$. The heat-transfer coefficient associated with this resistance is evaluated using Eq. 19. It is important to note that the area is normalized using the specific interfacial area of the bubbles. We have

$$q_{sensible} = \frac{\theta_2}{R_{sensible}} \tag{29}$$

$$\frac{1}{h_t A} = R_{sensible} \tag{30}$$

$$h_t = Le_f \cdot (\rho \bar{c}_{p,g} k_l) \cdot \frac{a_s \text{vol}}{A} \tag{31}$$

The specific interfacial area is evaluated using the following widely used expression[37]

$$a_s = \frac{6\epsilon}{D_b} \tag{32}$$

The associated log mean temperature difference is defined between the column temperature and the air inlet/exit temperature

$$\theta_2 = \frac{(T_{air,in} - T_{column}) - (T_{air,out} - T_{column})}{\ln\left(\frac{T_{air,in} - T_{column}}{T_{air,out} - T_{column}}\right)} \tag{33}$$

The latent heat-transfer rate is calculated using the following expression based on mass flux

$$q_{latent} = j \cdot h_{fg} \tag{34}$$

The mass flux is evaluated using the mass conversation equation across the bubble column condenser

$$j = \frac{\dot{m}_{da}}{A}(\omega_{in} - \omega_{out}) \tag{35}$$

The energy balance between the coolant and the air is written as follows

$$q = \frac{\dot{m}_{coolant} c_{p,coolant}}{A}(T_{coolant,out} - T_{coolant,in}) \tag{36}$$

$$= \frac{\dot{m}_{da}}{A}(h_{air,in} - h_{air,out}) \tag{37}$$

By applying a mass balance on the vapor over an incremental time dt and integrating the same over a residence time for the bubble in the liquid t_f we obtain the following expression.

$$k_l \cdot a_s = \frac{1}{t_f} \ln\left[\frac{\omega_{in} - \omega_{sat}}{\omega_{out} - \omega_{sat}}\right] \tag{38}$$

where the bubble residence time t_f is evaluated as the ratio of the liquid height and the bubble velocity

$$t_f = \frac{H}{V_b} \tag{39}$$

By solving Eqs. 25–39, we can obtain the heat flux and the associated temperatures from the estimated thermal resistance (Eqs. 5–24).

Solution technique

The equations presented in this section are solved simultaneously using Engineering Equation Solver (EES).[44] Water is used as the coolant in the coils, and EES evaluates water properties using the International Association for Properties of Water and Steam 1995 Formulation.[45] The vapor–gas mixture considered in this article is moist air, and its properties are evaluated assuming an ideal mixture of air and steam using the formulations presented by Hyland and Wexler.[46] Moist air properties from EES are in close agreement with the data presented in ASHRAE Fundamentals[47] and pure water properties are equivalent to those found in NIST's property package, REFPROP.[48] Dry air properties are evaluated using the ideal gas formulations presented by Lemmon et al.[49]

Experimental Details

A laboratory scale test rig was designed and built to study the condensation process from a vapor–air mixture in a bubble column condenser. Figure 4 shows a schematic diagram of the test apparatus used in the study. The apparatus consists of two bubble columns (4) and (9) with dimensions of

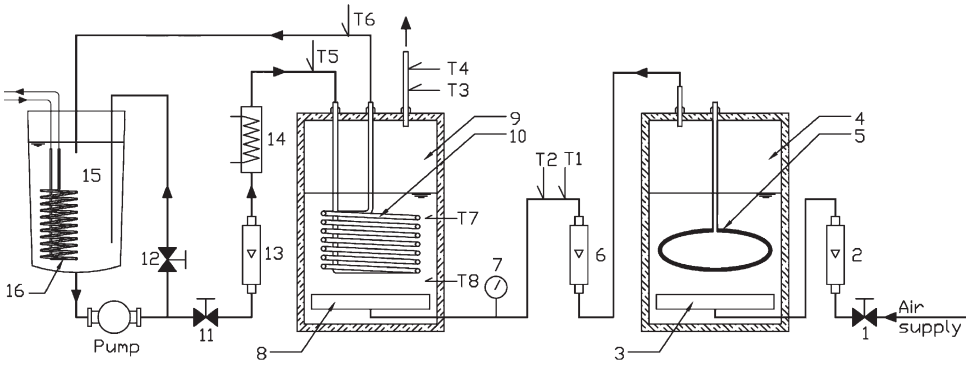

Figure 4. Schematic diagram of test apparatus: (1, 11, and 12) valves, (2, 6, and 13) rotameter, (3 and 8) sparger, (4) humidifier column, (5) submerged electric heater, (7) pressure gauge, (9) dehumidifier column, (10) water coil, (14) inline water heater, (15) cooling water tank, (16) chilled water coil, and (T1–T8) thermocouples.

12 in. (304.8 mm) width × 12 in. (304.8 mm) length × 18 in. (457.2 mm) height made from transparent poly vinyl cholride (PVC) sheets of 3/8 in. (9.52 mm) thickness. The first column (4) is used to produce moist air for the experiment by passing air through a sparger (3) into hot water. The water in this column is heated by a 1.5 kW submerged electric heater (5). The air is supplied from a compressor, and the flow rate is controlled by valve (1) and measured by rotameter (2). The humidified air from the first bubble column flows to the test column (9) where the dehumidification measurements are carried out. Before entering the second column, the flow rate is measured by a rotameter (6), the pressure is measured by a pressure gauge (7), and the dry and wet bulb temperatures are measured with thermocouples T1 and T2, respectively. Air flows into the sparger of the test column (8) where it is cooled and dehumidified using the cold copper coil (10). The copper coil has a pipe diameter of 1/4 in. (6.35 mm), a coil height of 6 in. (152.4 mm), and a turn diameter of 9 in. (228.6 mm). Cold water acting as the coolant flows inside the coil and is pumped from the cooling tank (15) where chilled water coil (16) keeps the temperature inside this tank almost constant. The dry bulb temperature and wet bulb temperature of the outlet air from the second column are measured by thermocouples T3 and T4, respectively. The two columns are provided with a charging and empting valve at the back side (not shown in the figure). Cold water from the cooling water tank (15) is pumped into the copper coil (10). The flow rate of the water is adjusted by the inline valve (11) and the bypass valve (12). The flow rate of water is measured by rotameter (13) and the fine temperature of the water can be adjusted by the inline electric water heater (14). The inlet and outlet water temperature from the copper coil are measured by thermocouples T5 and T6, respectively. The water temperature in the condenser bubble column is measured at two levels using thermocouples T7 and T8.

The sparger (3) of the humidifier bubble column (4) is a cartridge type sparger of 10 in. (254 mm) length. The sparger is from Mott corporation made of stainless steel (316LSS) porous pipe of 2 in. (50.8 mm) outside diameter and 1/16 in. (1.59 mm) thickness. This sparger generates uniform and fine bubble sizes and has a pressure drop less than 13.7 kPa (2 psi). The sparger (8) in the dehumidifier column is made of aluminum box 10 in. (254 mm) × 10 in. (254 mm) × 1 in. (25.4 mm). The top cover of this box is made of an acrylic sheet with a number of holes drilled in it to generate the air bubbles. There are five acrylic sheets; each one has different number of holes, hole diameter, and hole pitch as shown in Table 1. The thermocouples used in the apparatus are of K-type that are connected to a data logger and a laptop computer. The thermocouples and the data logging system have an uncertainty of ±0.1°C. The rotameters used for air flow measurements have a range of 0.8–8.2 ft^3/min (378–3870 cm^3/s) with a least count of ±0.2 ft^3/min (±94.4 cm^3/s). The rotameter used for water flow measurement has a range of 0.01–0.85 L/min with a least count of 0.01 L/min.

To study the impact of bubble-on-coil, we designed a set of circular coils to avoid impact and a set of serpentine coils that will facilitate impact. The photographs of the two set of coils are shown in Figure 5. The circular coil has a turn diameter of 9 in. (228.6 mm), and the sparger face area is 8 in. (203.2 mm) × 8 in. (203.2 mm), which brings the point of inception of the bubble to be vertically away from the coil. This helps minimize impact. In the serpentine coil, each pass of the coil is deliberately made to cross over the sparger holes maximizing impact. The results are markedly different for the two coils and are reported later on in this article (see "Effect of Bubble-on-Coil Impact" section).

Results and Discussion

In this section, we explain the importance of parameters such as superficial velocity, inlet mole fraction of vapor, bubble diameter, liquid column height, and effect of bubble-on-coil impact on the performance of a bubble column dehumidifier by varying these parameters independently.

The performance parameter of interest is the total heat flux exchanged between the coolant and the air–vapor mixture. Other alternative performance parameters, such as an "equivalent" heat-transfer coefficient, are not strictly correct, in contrast to the situation for a heat exchanger. This is because defining a global value for heat-transfer coefficient will involve defining a log mean temperature difference (or

Table 1. Sparger Design

Design No.	Hole Size (mm)	Pitch (mm)	Number of Holes
1	1.59	16	121
2	2.38	23	64
3	3.18	26	36
4	3.96	32	25
5	4.76	40	16

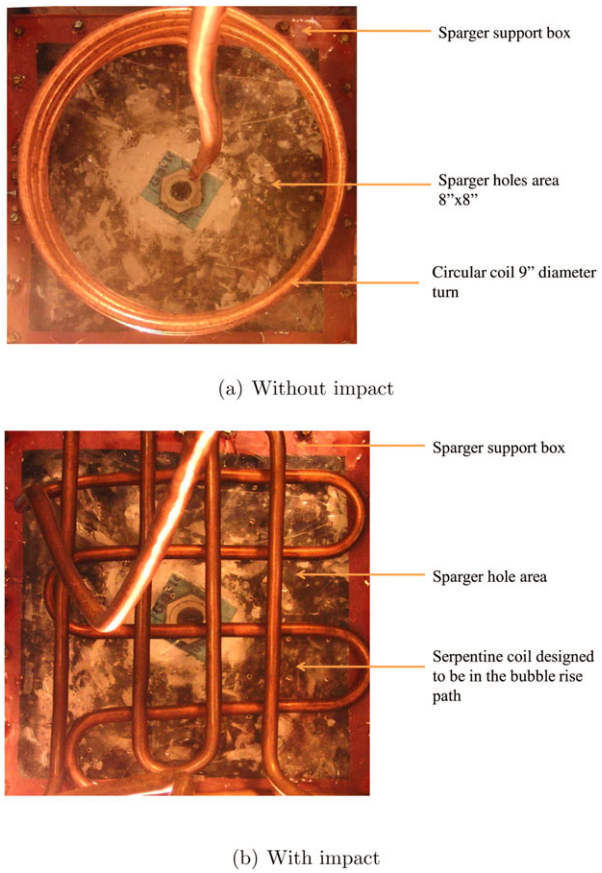

Figure 5. Photographs showing design of sparger and coil for (a) nonimpact and (b) impact cases.

[Color figure can be viewed in the online issue, which is available at wileyonlinelibrary.com]

another such global parameters for the device in its entirety) between the air and water temperatures at the inlet and outlets. This would amount to associating the mass transfer (and the associated latent heat release, which is the major portion of the total heat exchanged between the fluid streams) with a temperature difference; this is of course inappropriate, because the mass transfer is associated with a concentration difference and not a temperature difference.[50–52] It is, hence, logical to use heat flux as the performance parameter, because it captures all the important characteristics of the bubble column dehumidifier (including the condensation rate) but does not involve all of the aforementioned issues.

Effect of superficial velocity

Several researchers have studied the effect of superficial velocity on mass transfer in bubble columns.[19,53–56] These studies, however, did not involve condensation from the bubble into the liquid column. A typical example of the mass-transfer studies in the literature would be absorption of isobutylene in aqueous solutions of H_2SO_4.[57,58] Researchers have also separately studied the effect of superficial velocity on heat transfer to immersed surfaces in bubble column reactors.[23,24,25,59–64] However, we should note that the effect of superficial velocity on simultaneous heat and mass exchange with condensation has not been studied before (to the best knowledge of the authors), and it will be the focus of this section.

The general consensus in the literature is that the heat- and mass-transfer coefficients are higher at higher superficial velocity.[65] Studies have also shown that the rate of increase of heat-transfer coefficients with gas velocity is more pronounced at lower gas velocity and more gradual at higher gas velocities. This is due to the change in flow regime from homogenous bubbly flow to the churn-turbulent regime. The effect of increase in superficial velocity is reported to be lower in the churn-turbulent regime.

A flow regime map reported by Shah and Sekulić[19] predicts that the transition velocity for the experimental bubble column reported in the current publication lies somewhere between 4.5 and 7 cm/s (based on an effective column diameter of 30.5 cm). During experimentation, it was observed that between superficial velocities of 3 and 8 cm/s the bubble flow was either perfect or imperfect bubbly flow (churn turbulence and slug flow were not observed).

Figure 6 illustrates experimental and calculated values of heat flux at various values of superficial velocity. These results are at fixed values for bubble diameter, inlet mole fraction, and water column height. The trend and the slope of the curve presented in Figure 6 is representative of the trend obtained at other values of the aforementioned fixed parameters. From Figure 6, it may be observed that as the superficial velocity was increased, the heat flux was increased, which is a conclusion consistent with other such studies in the literature. In addition, it can be observed that the predictive model estimates the effect of the superficial velocity accurately.

The uncertainty of measurement on the superficial velocity is ± 0.11 cm/s and that on the heat flux is $\pm 5\%$.

Effect of bubble diameter

In the literature, no consensus is evident on the effect of bubble diameter on transport coefficients in bubble columns. On the one hand, some researchers have reported that bubble properties (including bubble diameter) affect the mass-transfer coefficient greatly,[66–68] on the other hand, Deckwer[23] has suggested that there is no evidence of the effect of bubble diameter on heat transfer to immersed surfaces. Also, the effect of bubble diameter on simultaneous heat and mass transfer has not been investigated yet.

Our experiments and modeling show (see Figure 7) that there is a relatively minor but discernible effect of bubble

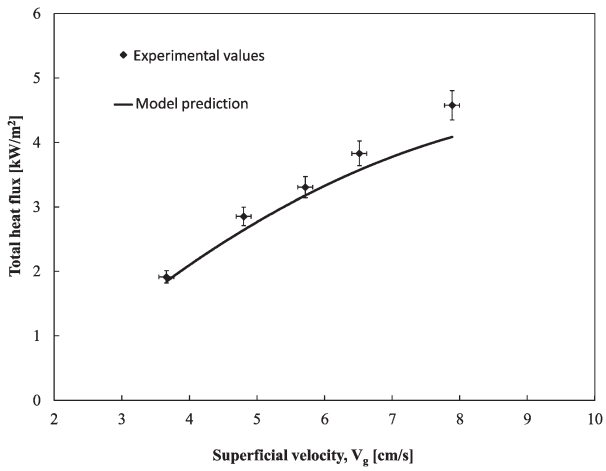

Figure 6. Effect of superficial velocity on the total heat flux in the bubble column measured and evaluated at $D_b = 4$ mm; $\chi_{in} = 21\%$; $H = 254$ mm.

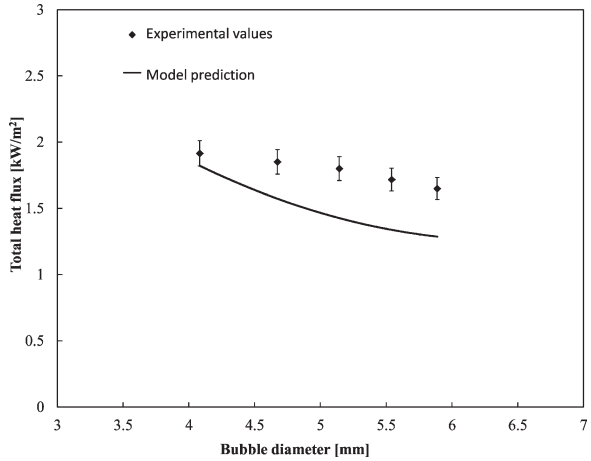

Figure 7. Effect of bubble diameter on the total heat flux in the bubble column measured and evaluated at $V_g = 3.8$ cm/s; $\chi_{in} = 21\%$; $H = 254$ mm.

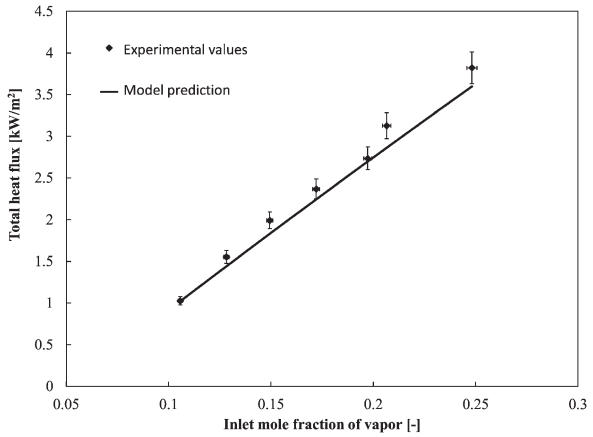

Figure 8. Effect of inlet mole fraction of the vapor on the total heat flux in the bubble column measured and evaluated at $V_g = 3.8$ cm/s; $D_b = 4$ mm; $H = 254$ mm.

diameter on the total heat flux exchanged in a bubble column dehumidifier. The heat flux is found to decrease with an increase in bubble diameter. This result is found to be consistent at other values of the fixed parameters (superficial velocity, inlet mole fraction, and liquid height) as well. It is to be noted that the predictive model proposed in "Predictive Model for Combined Heat and Mass Transfer" section predicts the trend in Figure 7 to a good degree of accuracy.

Effect of inlet mole fraction

In steam condensers with a small amount of noncondensable gas present (<10% by mole), the inlet mole fraction of vapor has been reported to have a very sharp effect on the heat-transfer coefficient.[10,14] As mentioned earlier (in "Introduction" section), experimental data in the literature suggest that the effect is almost quadratic in nature. In this section, we investigate the effect of the same parameter in a bubble column dehumidifier.

The inlet mole fraction of vapor is varied from 10 to 25% (3.6–9 times lower than regular condensers) at fixed values of superficial velocity, bubble diameter, and liquid height. Figure 8 illustrates the experimental and modeling results for the same. A strong effect of the mole fraction is seen, as is also the case in steam condensers. From our experiments, we observe that the effect is more linear than quadratic (in the studied range). Hence, the presence of noncondensable gas is affecting the heat transfer to a much lesser degree than in the film condensation situations of a standard dehumidifier. This demonstrates the superiority of the bubble column dehumidifier.[29] This observation is further discussed in "Comparison with Existing Devices" section. Figure 8 also illustrates that the predictive model predicts the effect of inlet mole fraction very accurately.

The uncertainty of measurement on the mole fraction is $\pm 1\%$.

Effect of liquid column height

Regular dehumidifiers and steam condensers can be designed to have minimal pressure drop (as low as a few hundred Pa). In bubble columns, a large percentage of the pressure drop that occurs on the vapor side is due to the hydrostatic head of the liquid in the column that the air–vapor mixture has to overcome. Thus, it is desirable to keep the liquid height to a minimum value. The cooling coils must remain fully immersed in the liquid pool, and hence, the minimum liquid height should be that which just immerses the coils.

Figure 9 illustrates that there is no effect of reducing the liquid height from 10 in. (254 mm) in 6 in. (152.4 mm—the minimum height at which the coil was fully immersed). This can be understood by considering the length scale of the liquid circulation, which we have postulated as the integral length of turbulence. As explained earlier in "Thermal Resistance Between the Liquid in the Column and the Coil Surface" section, the integral length is very close to the bubble diameter. Hence, the scale at which the circulation happens in the liquid is of the order of a millimeter, which is two orders of magnitude lower than the liquid height. Therefore, unless the liquid height is reduced to a few millimeters, it will not have an effect on the bubble column performance. This is a very significant consideration when designing bubble column dehumidifiers for systems, which cannot take large gas side pressure drops, such as the humidification dehumidification desalination (HDH) system.[69,70] The intricacies of integrating the bubble column dehumidifier with low liquid height in an HDH system are explained in a separate publication.[29]

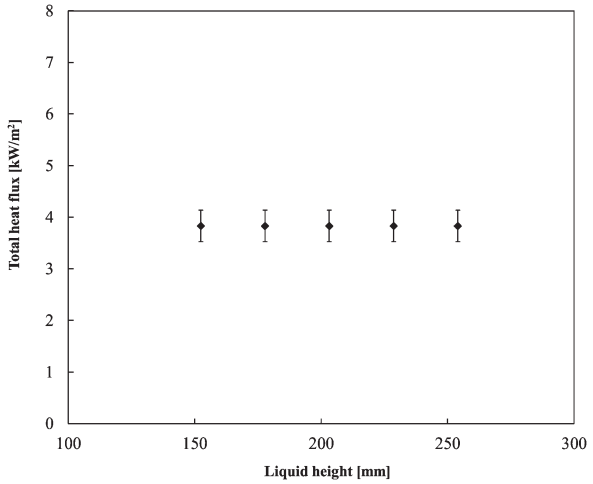

Figure 9. Effect of liquid height on the total heat flux in the bubble column measured and evaluated at $V_g = 6.52$ cm/s; $D_b = 4$ mm; $\chi_{in} = 21\%$.

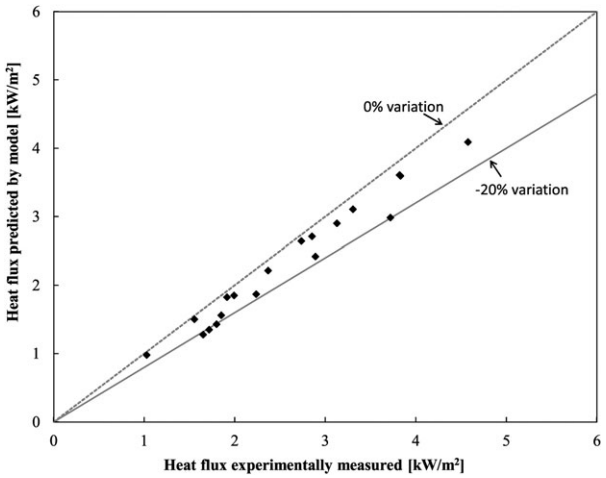

Figure 10. Parity plot of heat flux values evaluated by the model and that measured by experiments for various boundary conditions.

Comparison of model and experiments

We have seen that the predictive model estimates the effect of bubble diameter, superficial velocity, and inlet mole fraction of vapor on heat flux exchanged in a bubble column dehumidifier accurately. In Figure 10, we present a comparison of the experimental data and the model for various boundary conditions in a parity plot. There is excellent agreement (within −20%), and as per our expectation, the model consistently underpredicts the heat flux. This is because we approximated the boundary layer inside the bubble to be of the order of the bubble radius itself (''Thermal Resistance Between the Liquid in the Column and the Bubbles'' section), which is clearly an overestimation of the associated thermal resistance.

Effect of bubble-on-coil impact

In consideration of the effect of all of the different parameters (described in the previous paragraphs), bubble-on-coil impact was avoided during experimentation (see ''Experimental Details'' section) and neglected in the predictive model. In this section, we study the effect of impact using the serpentine coils shown in Figure 5. Figure 11 illustrates this effect. It may be observed that impact raises the heat-transfer rates to significantly higher values. Thus, in case of the serpentine coils, a major portion of the heat communicated between the air–vapor bubbles and the coils is through direct impact between the two. Hence, to obtain higher heat-transfer rates, it is desirable to design coils to have maximum impact.

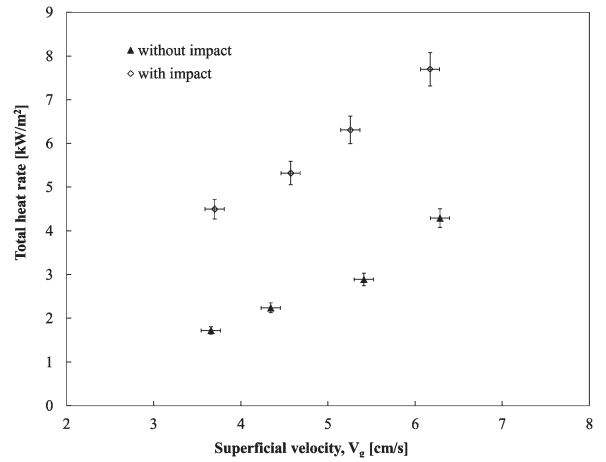

Figure 11. Effect of bubble-on-coil impact.

Comparison with existing devices

A state-of-the-art dehumidifier (which operates in the film condensation regime) procured from George Fischer LLC was found to yield a maximum heat flux of 1.8 kW/m^2 (as per the design specification) compared to a maximum of 8 kW/m^2 obtained in the bubble column dehumidifier (with high bubble-on-coil impact and a superficial velocity of 7 cm/s) demonstrating the superior performance of the novel device. This comparison has been carried out at the same inlet conditions for the vapor–air mixture and the coolant streams. Also, the streamwise temperature differences were similar in both the cases.

Concluding Remarks

This article has proposed a novel bubble column vapor–gas condenser (or dehumidifier) for condensation of vapor in the presence of a large percentage of noncondensable gas. The main conclusions are follows.

1. Bubble column dehumidifiers have an order of magnitude higher heat rates than existing state-of-the-art dehumidifiers operating in the film condensation regime.

2. The bubble column should be designed for high superficial velocity, low bubble diameter, and maximum bubble-on-coil impact. To minimize pressure drop, the liquid height can be kept to a minimum such that the coil is entirely submerged in the liquid. This is possible, because the height has no effect on the performance of the device if it is greater than the bubble diameter (≈4–6 mm).

3. The inlet mole fraction of the vapor is found to have a weaker effect on the performance of the device than in a regular dehumidifier (in which the performance deteriorates quadratically with the vapor mole fraction).

4. A physics based predictive heat-transfer model based on a thermal resistance circuit to estimate heat flux and temperature profiles in the bubble column condenser has been developed. The experimental data are predicted within −20%. The model accurately predicts the effects of the various parameters on heat flux without incorporating any adjustable parameters.

Acknowledgments

The authors thank the King Fahd University of Petroleum and Minerals for funding the research reported in this article through the Center for Clean Water and Clean Energy at MIT and KFUPM. S.K. Das thanks Massachusetts Institute of Technology for providing him with a Peabody Visiting Professorship that helped him participate in this study.

Notation

a_s = specific interfacial area of the bubble column, m^2/m^3
c = flexible constant used by Deckwer[23]
c_p = specific heat capacity at constant pressure, J/(kg K)
$c_{p,g}$ = average specific heat capacity at constant pressure of the vapor–air mixture, J/(kg K)
D_{AB} = diffusion coefficient, m^2/s
D_b = bubble diameter, m
d_o = sparger hole diameter, m
g = gravitational acceleration, m/s^2
H = liquid height in the column, m
h = heat-transfer coefficient, W/(m^2 K)
h_{air} = specific enthalpy of air–vapor mixture, J/kg dry air

h_{fg} = specific enthalpy of vaporization, J/kg
h_t = heat-transfer coefficient for the sensible heat exchanged between bubble and liquid column, W/m^2 K
j = mass flux, kg/m^2 s
k = thermal conductivity, W/m K
k_l = mass-transfer coefficient, m/s
l = characteristic length, m
l_{int} = integral length for turbulence, m
$\dot{m}$ = mass flow rate, kg/s
n = exponent
q = heat flux, W/m^2
q_{lt} = heat flux due to condensation of vapor from the bubble in the liquid column, W/m^2
$q_{lt,impact}$ = heat flux due to direct condensation of vapor from the bubble on the coil surface, W/m^2
$q_{sensible}$ = heat flux due to the sensible heat exchange between bubble and liquid column, W/m^2
R = thermal resistance, (K m^2)/W
R_{bc} = thermal resistance between the liquid column and the coil surface, (K m^2)/W
R_{coil} = thermal resistance due to coolant flow inside the coil, (K m^2)/W
R_{bc} = thermal resistance between the liquid column and the coil surface, (K m^2)/W
R_m = mass-transfer resistance, (s m^2)/kg
$R_{sensible}$ = thermal resistance for the sensible heat exchange between bubble and liquid column, K m^2/W
t = surface renewal time, s
t_f = average residence time of the bubble in the liquid, s
T = temperature, °C
T_{air} = local energy-averaged temperature of the air–vapor bubble, °C
T_{coil} = local temperature of the coil surface, °C
T_{column} = local energy-averaged temperature of the liquid in the column, °C
$T_{coolant}$ = local energy-averaged temperature of the coolant in the coil, °C
u = velocity in the x direction, m/s
V = velocity, m/s
V_b = bubble velocity, m/s
V_c = circulation velocity, m/s
V_g = superficial velocity, m/s
V_r = radial velocity in the liquid column, m/s
vol = volume of the bubble column, m^3

Greek letters

α = thermal diffusivity, m^2/s
∂ = operator for partial derivative
ϵ = volumetric gas holdup
ε = turbulent energy dissipation rate per unit mass, m^2/s^3
θ = log mean temperature difference, K
ν = kinematic viscosity, m^2/s
ρ = density, kg/m^3
σ = surface tension, N/m
ω = absolute humidity, kg water vapor/kg dry carrier gas
χ = mole fraction

Subscripts

da = dry air
l = liquid
g = gas
in = inlet
out = outlet
sat = saturated

Nondimensional numbers

Fr = Froude number, $V_g^2/(g \cdot D_b)$
Le = Lewis number, α/D_{AB}
Le_f = Lewis factor, $h_t/(\rho c_{p,g} k_l)$
Pr = Prandtl number, ν/α
Re = Reynolds number, $(V_g \cdot D_b)/\nu$
St = Stanton number, $h/(\rho c_p V_g)$

Literature Cited

1. Colburn AP, Hougen OA. Design of cooler condensers for mixtures of vapors with noncondensing gases. *Ind Eng Chem*. 1934;26:1178–1182.
2. Nusselt W. Die oberflachenkondensation des wasserdampfes. *Zeitschrift des VereinsDeutscherIngenieure*. 1916;60:541–546.
3. Sparrow EM, Eckert ERG. Effects of superheated vapor and noncondensable gases on laminar film condensation. *AIChE J*. 1961;7:473–477.
4. Sparrow EM, Minkowycz WJ, Saddy M. Forced convection condensation in the presence of noncondensables and interfacial resistance. *Int J Heat Mass Transfer*. 1967;10:1829–4745.
5. Minkowycz WJ, Sparrow EM. Condensation heat-transfer in the presence of noncondensables: interfacial resistance, superheating, variable properties, and diffusion. *Int J Heat Mass Transfer*. 1966;9:1125–1144.
6. Denny VE, Mills AF, Jusionis VJ. Laminar film condensation from a steam–air mixture undergoing forced flow down a vertical surface. *J Heat Transfer*. 1971;93:297–304.
7. Denny VE, Jusionis VJ. Effects of noncondensable gas and forced flow on laminar film condensation. *Int J Heat Mass Transfer*. 1972;15:315–326.
8. Wang CY, Tu CJ. Effects of non-condensable gas on laminar film condensation in a vertical tube. *Int J Heat Mass Transfer*. 1988;31:2339–2345.
9. Kageyama T, Peterson PF, Schrock VE. Diffusion layer modeling for condensation in vertical tubes with noncondensable gases. *Nuclear Eng Des*. 1993;141:289–302.
10. Hasanein HA. Steam condensation in the presence of noncondensable gases under forced convection conditions. Ph.D. thesis, Massachusetts: Institute of Technology, 1994.
11. Kuhn SZ. Investigation of heat-transfer from condensing steam–gas mixture and turbulent films flowing downward inside a vertical tubes. Ph.D. thesis, University of California, Berkeley, 1995.
12. Maheshwari NK, Vijayan PK, Saha D. Effects of non-condensable gases on condensation heat-transfer. In: *Proceedings of 4th RCM on the IAEA CRP on Natural Circulation Phenomena*, 2007, Vienna Austria (Sept. 10–13, 2007).
13. Hasanein HA, Kazimi MS, Golay MW. Forced convection in-tube steam condensation in the presence of noncondensable gases. *Int J Heat Mass Transfer*. 1996;39:2625–2639.
14. Siddique M, Golay MW, Kazimi MS. *Local heat-transfer coefficients for forced convection condensation of steam in a vertical tube in the presence of air*. *Two-Phase Flow and Heat Transfer*, 3rd ed., Vol. 197. New York: ASME, 1992:386–402.
15. Rao VD, Krishna VM, Sharma KV, Rao PM. Convective condensation of vapor in the presence of a non-condensable gas of high concentration in laminar flow in a vertical pipe. *Int J Heat Mass Transfer*. 2008;51:6090–6101.
16. Hamieh BM, Beckman JR, Ybarra MD. Brackish and seawater desalination using a 20 sq. ft. dewvaporation tower. *Desalination*. 2001;140:217–226.
17. Hamieh BM, Beckman JR. Seawater desalination using dewvaporation technique: experimental and enhancement work with economic analysis. *Desalination*. 2006;195:14–25.
18. Degaleesan S, Dudukovic M, Pan Y. Experimental study of gas-induced liquid-flow structures in bubble columns. *AIChE J*. 2001;47:1913–1931.
19. Shah RK, Sekulić DP. *Fundamentals of Heat Exchanger Design*. Wiley, 2003.
20. Hulet C, Clement P, Tochon P, Schweich D, Dromard N, Anfray J. Heat transfer in two- and three-phase bubble columns. *Int J Chem Reactor Eng*. 2009;7:1–93.
21. Kulkarni AV, Joshi JB. Design and selection of sparger for bubble column reactor. Part I: Performance of different spargers. *Chem Eng Res Des*. 2011;89:1972–1985.
22. Joshi JB, Sharma MM. A circulation cell model for bubble columns. *Chem Eng Res Des*. 1979;57a:244–251.
23. Deckwer WD. On mechanism of heat-transfer in bubble column reactors. *Chem Eng Sci*. 1980;35:1341–1346.
24. Konsetov VV. Heat transfer during bubbling of gas through liquid. *Int J Heat Mass Transfer*. 1966;9:1103–1108.
25. Kast W. Analyse des wrmebergangs in blasensulen. *Int J Heat Mass Transfer*. 1962;5:389–350.
26. Kutateladze SS, Styrikovich MA. *Hydraulics of gas–liquid systems*. Wright-Patterson Air Force Base, 1960.
27. Kolmogorov A. On degeneration of isotropic turbulence in an incompressible viscous liquid. *Doklady Akademiia Nauk SSSR*. 1941;31:538–540.
28. Higbie R. The rate of absorption of a pure gas into a still liquid during a short time of exposure. *Trans Am Inst Chem Eng*. 1935;35:365–389.

29. Narayan GP, Thiel GP, McGovern RK, Sharqawy MH, Lienhard JH V. Multi-stage bubble column dehumidifier. Patent pending, USSN # 13/241,907, 2011.
30. Dias NL, Chamecki M, Kan A, Okawa CMP. Study of spectra, structure and correlation functions and their implications for the stationarity of surface-layer turbulence. *Boundary Layer Meteorol*. 2004;110:165–189.
31. Tritton DJ. *Physical Fluid Dynamics*. Oxford University Press, 1988.
32. I'Aglom AM. *Correlation Theory of Stationary and Related Random Functions, Vol 1: Basic Results*. Springer Verlag, 1987.
33. ONeill PL, Nicolaides D, Honnery D, Soria J. Autocorrelation functions and the determination of integral length with reference to experimental and numerical data. In: *Proceedings of 15th Australasian Fluid Mechanics Conference*. Dec. 13–17, 2004, The University of Sydney; Paper # AFMC00064:1–3.
34. Magaud F, Souhar M, Wild G, Boisson N. Experimental study of bubble column hydrodynamics. *Chem Eng Sci*. 2001;56:4597–4607.
35. Souhar M. Some turbulence quantities and energy spectrain the wall region in bubble flows. *Phys Fluids A*. 1989;1:1558–1565.
36. Lance M, Bataille J. Turbulence in the liquid phase of a uniform bubbly air–water flow. *J Fluid Mech*. 1991;222:95–118.
37. Miller DN. Scale-up of agitated vessels gas–liquid mass-transfer. *AIChE J*. 1974;20:445–453.
38. Field RW, Rahimi R. *Hold-up heat-transfer in bubble columns*. In: *Fluid Mixing III*. Amarousion-Pefki, Greece: European Federation of Chemical Engineering, 1988:257–270.
39. Mendelson HD. The prediction of bubble terminal velocities from wave theory. *AIChE J*. 1967;13:250–258.
40. Merkel F. *Verdunstungskuhlung*. In: *VDI Forschungsarbeiten*. Berlin, 1925;275.
41. Threlkeld JL. *Thermal Environmental Engineering*. Prentice-Hall, Inc. 1970.
42. Bosnjakovic F. *Technische Thermodinamik*. Dresden: Theodor Steinkopf, 1965.
43. Lienhard JH IV, Lienhard JH V. *A Heat Transfer Text Book*. Cambridge, MA: Phlogiston Press, 2008.
44. Klein SA. Engineering Equation Solver, Academic Professional, Version 8. 2009. Available at: http://www.fchart.com/.
45. Pruss S, Wagner W. The IAPWS formulation 1995 for the thermodynamic properties of ordinary water substance for general and scientific use. *J Phys Chem Ref Data*. 2002;31:387–535.
46. Hyland RW, Wexler A. Formulations for the thermodynamic properties of dry air from 173.15 K to 473.15 K, and of saturated moist air from 173.15 K to 372.15 K, at pressures to 5 MPa. *ASHRAE Trans*. 1983;2794(Pt 2A)(RP-216):520–535.
47. Wessel DJ. *ASHRAE Fundamentals Handbook 2001 (SI Edition)*. American Society of Heating, Refrigerating, and Air-Conditioning Engineers, 2001.
48. Lemmon EW, Huber ML, McLinden MO. NIST Standard Reference Database 23: reference fluid thermodynamic and transport properties. *Tech. Rep*., REFPROP. Version 8.0, 2007.
49. Lemmon EW, Jacobsen RT, Penoncello SG, Friend DG. Thermodynamic properties of air and mixtures of nitrogen, argon, and oxygen from 60 to 2000 K at pressures to 2000 MPa. *J Phys Chem Ref Data*. 2000;29(3):331–385.
50. Thiel GP, Lienhard JH V. Entropy generation in condensation in the presence of high concentrations of noncondensable gases. *Int J Heat Mass Transfer*. 2012;55:5133–5147.
51. Narayan GP, Mistry KH, Sharqawy MH, Zubair SM, Lienhard JH V. Energy effectiveness of simultaneous heat and mass exchange devices. *Front Heat Mass Transfer*. 2010;1:1–13.
52. Narayan GP, Lienhard JH V, Zubair SM. Entropy generation minimization of combined heat and mass-transfer devices. *Int J Thermal Sci*. 2010;49:2057–2066.
53. Schumpe A, Grund G. The gas disengagement technique for studying gas holdup structure in bubble columns. *Can J Chem Eng*. 1986;64:891–896.
54. Ozturk SS, Schumpe A, Deckwer WD. Organic liquids in a bubble column: holdups and mass-transfer coefficients. *AIChE J*. 1987;33:1473–1480.
55. Akita K, Yoshida F. Gas hold-up and volumetric mass-transfer coefficients in bubble columns. *Ind Eng Chem Process Des Dev*. 1973;12:76–80.
56. Kang Y, Cho YJ, Woo KJ, Kim SD. Diagnosis of bubble distribution and mass-transfer in pressurized bubble columns with viscous liquid medium. *Chem Eng Sci*. 1999;54:4887–4896.
57. Gehlawat JK, Sharma MM. Absorption of isobutylene in aqueous solutions of sulfuric acid. *Chem Eng Sci*. 1968;23:1173–1186.
58. Kroper H, Schlomer K, Weitz HM. How BASF extracts isolentylene. *Hydrocarbon Process*. 1969;195:1–7.
59. Hikita H, Asal S, Kikukawa H, Zalke T, Ohue M. Heat transfer coefficients in bubble column. *Ind Eng Chem Process Des Dev*. 1981;20:540–545.
60. Kawase Y, Moo-Young M. Heat transfer in bubble column reactors with Newtonian and non-Newtonian fluids. *Chem Eng Res Des*. 1987;65:121–126.
61. Kato Y, Uchida K, Kago T, Morooka S. Liquid holdup and heat transfer coefficient between bed and wall in liquid–solid and gas–liquid–solid fluidized beds. *Powder Technol*. 1981;28:173–179.
62. Cho YJ, Woo KJ, Kang Y, Kim SD. Dynamic characteristics of heat-transfer coefficient in pressurized bubble columns with viscous medium. *Chem Eng Process*. 2002;41:699–706.
63. Saxena SC, Rao NS, Saxena AC. Heat-transfer and gas-holdup studies in a bubble column: air–water–glass bead system. *Chem Eng Commun*. 1990;96:31–55.
64. Li H, Prakash A. Heat transfer and hydrodynamics in a three-phase slurry bubble column. *Ind Eng Chem Res*. 1997;36:4688–4694.
65. Kantarci N, Borak F, Ulgen KO. Bubble column reactors. *Process Biochem*. 2005;40:2263–2283.
66. Fukuma M, Muroyama K, Morooka S. Properties of bubble swarm in a slurry bubble column. *J Chem Eng Jpn*. 1987;20:28–33.
67. Krishna R, Baten JMV. Mass transfer in bubble columns. *Catal Today*. 2003;79–80:67–75.
68. Behkish A, Men Z, Inga RJ, Morsi BI. Mass transfer characteristics in a large-scale slurry bubble column reactor with organic liquid mixtures. *Chem Eng Sci*. 2002;57:3307–3324.
69. Narayan GP, Sharqawy MH, Summers EK, Lienhard JH V, Zubair SM, Antar MA. The potential of solar-driven humidification-dehumidification desalination for small-scale decentralized water production. *Renew Sustain Energy Rev*. 2010;14:1187–1201.
70. Narayan GP, Sharqawy MH, Lienhard JH V, Zubair SM. Thermodynamic analysis of humidification dehumidification desalination cycles. *Desalination Water Treat*. 2010;16:339–353.

Manuscript received Mar. 6, 2012, and revision received Aug. 30, 2012.